LASER INTERFEROMETER GRAVITATIONAL WAVE OBSERVATORY
-LIGO-
CALIFORNIA INSTITUTE OF TECHNOLOGY
MASSACHUSETTS INSTITUTE OF TECHNOLOGY

Technical Note **LIGO-T040156- 00- E** 9/22/2004

Mirror Reflective Phase-Maps for FFT Simulation

Xiao Xu (Caltech 2004 SURF),
Hiroaki Yamamoto (Caltech LIGO)

This is an internal working note
of the LIGO Project.

California Institute of Technology
LIGO Project - MS 18-34
Pasadena CA 91125
Phone (626) 395-2129
Fax (626) 304-9834
E-mail: info@ligo.caltech.edu

Massachusetts Institute of Technology
LIGO Project - MS NW17-161
Cambridge, MA 02139
Phone (617) 253-4824
Fax (617) 253-4824
E-mail: info@ligo.mit.edu

WWW: http://www.ligo.caltech.edu/

file /home/xxu/public_html/pdf/T040156.pdf

Introduction

LIGO is currently in the commissioning phase. The scientists and engineers at the sites are constantly finetuning the interferometers. Despite the high demanding of precision and sensitivity, LIGO, composed of six mirrors, has various innate defects; one of them is the imperfection of the mirror surfaces. As designed, all mirrors should have perfectly smooth surfaces. However, as manufactured, mirror surfaces have a roughness of the order of nanometer. No one knows what kind of noise will this surface roughness introduces. Yet the people at the sites have observed some mysterious noises, which they suspect are attribute to the imperfection of mirror surfaces.

To assist the efforts at the sites, several computer programs are wrote to simulate the operation of LIGO. FFT program [1] is one of such programs, which staticly simulate the steady state of the E&M fields within the interferometer. Thus, FFT program is an ideal tool to test the effects of the imperfection of mirror surfaces. In order to model actual mirrors at LIGO, FFT program needs the input of reflective phase-maps and transmissive phase-maps. However, due to techniqual issues, transmissive phase-maps are very difficult, if not impossible, to measure. Only the reflective phase-maps have been measured at Caltech [2]. Yet, we guess that the effects of transmissive phase-maps have the same order of magnitude as that of reflective ones. Therefore, the reflective phase-maps are of great importance to the estimation of noises caused by mirror surface aberration.

Data Conversion

For each mirror, reflective phase-map of the central region, a disc with diameter $150\ (mm)$, has been measured. The measured phase-maps can be represented by 480×576 matrices[1]. The size of every cell of the matrices is $0.266800 \times 0.311356\ (mm^2)$. Since, FFT program uses *Fast Fourier Transformation*, the input data must be square matrix with dimensions of powers of 2, such as matrices of dimensions 128×128 or 256×256. Therefore, the measured data need to be converted into the required format.

As indicated by Fig 1, the scheme which converts an $n \times m$ matrix, with a cell size $dm \times dn$, to a coarser $N \times N$ matrix, with cell size $dN \times dN$, is as follows [3]:

1. Impose the coarser matrix onto the finer one with the reference of a coordinate system.

[1]The data outside the measured circular region are marked as "Bad". Before processing the data conversion, all values marked as "Bad" are substituted by zero.

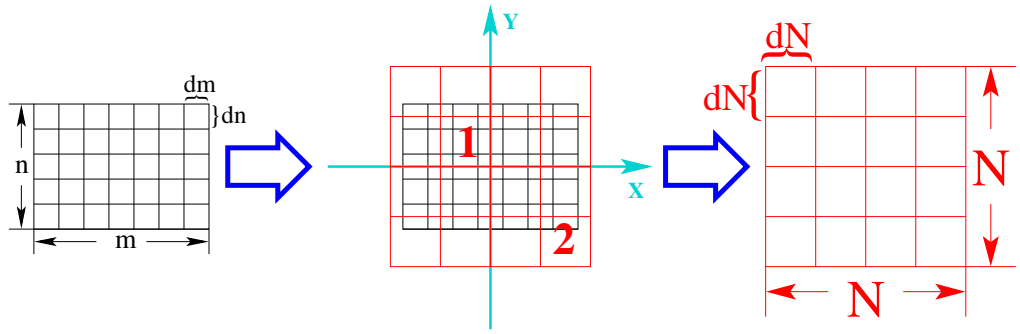

Figure 1: The Schematic Diagram of Conversion of Input Matrices

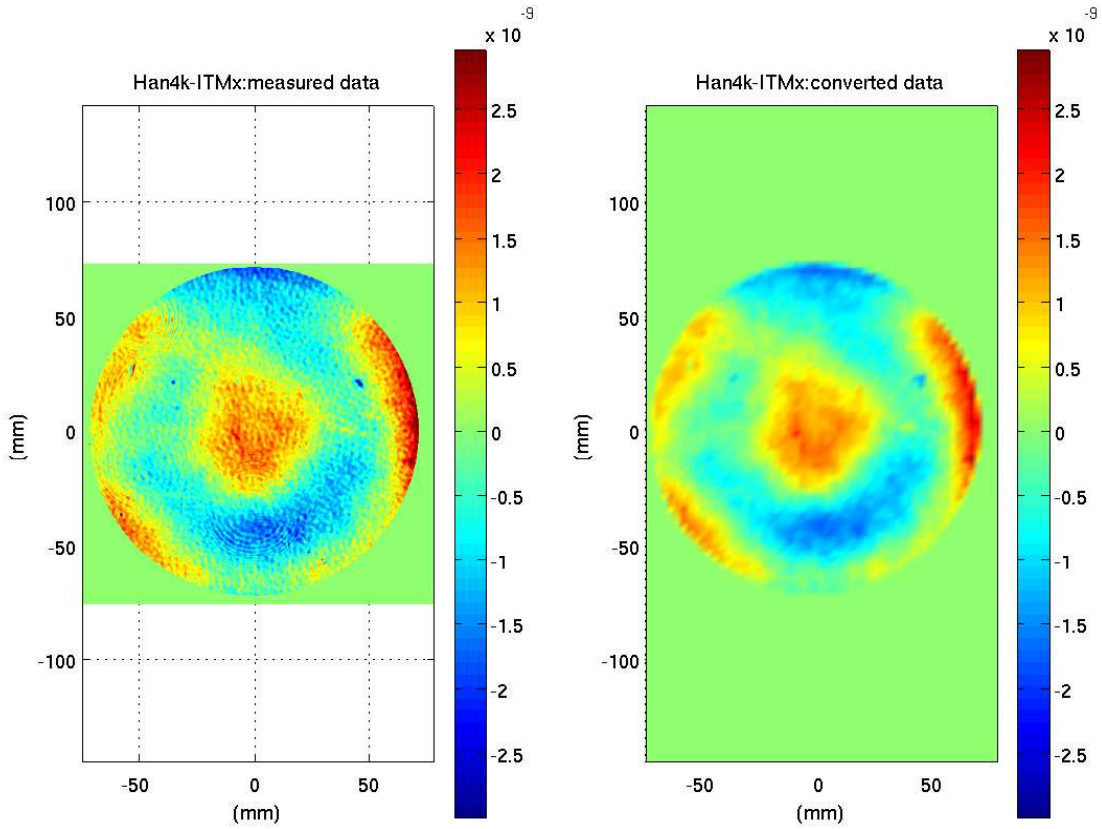

Figure 2: Example of Data conversion

2. If a cell of the coarser matrix is completely inside the finer matrix, such as cell 1 in Fig 1, then the value assigned to this cell is the weighted average of the values of the finer matrix enclosed by this cell. The weight of each value of the finer matrix is proportional to the area of this value which is within the boundary of the cell of the coarser matrix.

3. If a cell of the coarser matrix is partially or completely outside the finer matrix, such as cell 2 in Fig 1, then set the value of the area outside the finer matrix to be zero, and assign the cell weighted average of the values enclosed by it.

By such method, the measured phase-maps, 480×576 matrices with cell size $0.266800 \times 0.311356\ (mm^2)$, have been converted to the required formats, 128×128 matrices with cell size $2.734375 \times 2.734375\ (mm^2)$[2] (Fig 2).

Extrapolation

In order to model an actual mirror with the coated circular area with $24\ (cm)$ diameter, the measured data within a circular area with $15\ (cm)$ diameter need to be extrapolated. Strictly speaking, there is no way to predict the phasemap in the unmeasured region. The best one can do is to extrapolate reasonably based on an educated guess[3].

Zernike Fit

The basic assumption is that the smooth structures of the phasemap up to 2nd order, i.e., piston, x-tilt, y-tilt, power, astigmatisms, are universal on the entire mirror surface. The measured phasemap is fit by using the 37 Wyko polynomials, and the coefficient of the first 6 Wyko polynomials [4] are used to smoothly extrapolate the phasemap. The Wyko polynomials is a particular set of the Zernike Polynomials [4], which are commonly used to describe the surface aberration of optics. The fitting coefficients can be found by minimizing χ^2, that's to minimize the following:

$$\chi^2 = \sum_i \sum_j \Big(\frac{f(x_i, y_j) - z(x_i, y_j)}{\sigma_{ij}^2} \Big)^2 \ , \text{ with} \tag{1}$$

[2]The converted matrix covers a $35 \times 35\ (cm^2)$ area.

[3]The systematic errors of simualtion results are estimated by comparing results using phasemaps based on this extrapolation and results using phasemaps based on another assumption. This will be discussed in a separated document LIGO-T040173-00-E [7].

$$f(x_i, y_j) = \sum_k a_k w_k(\hat{x_i}, \hat{y_j}) \ , \tag{2}$$

$$\hat{x_i} = \frac{x_i}{r} \ , \ \ \hat{y_j} = \frac{y_j}{r} \ , \tag{3}$$

where (i, j) is the index of measured data points, $z(x, y)$ is the measured data, $f(x, y)$ is the fitting function with $\{a_k\}$ the fitting coefficient, σ_{ij} is the standard deviation of each measurement, $w_k(\hat{x}, \hat{y})$ is the Wyko Polynomials serving as the basis of the fitting, and r is the radius of the measured phasemap, ie. $7.5(cm)$.

Differentiate equation (1) with respect to $\{a_k\}$, it becomes

$$\frac{\partial \chi^2}{\partial a_k} = \sum_i \sum_j 2 w_l(\hat{x_i}, \hat{y_j}) \Big(\frac{f(x_i, y_j) - z(x_i, y_j)}{\sigma_{ij}^2} \Big) \ . \tag{4}$$

To minimize χ^2, equation (4) is set to equal zero. Thus,

$$\sum_i \sum_j w_l(\hat{x_i}, \hat{y_j}) \Big(\frac{f(x_i, y_j) - z(x_i, y_j)}{\sigma_{ij}^2} \Big) = 0 \tag{5}$$

$$\Rightarrow \sum_i \sum_j \frac{w_l(\hat{x_i}, \hat{y_j}) f(x_i, y_j)}{\sigma_{ij}^2} = \sum_i \sum_j \frac{w_l(\hat{x_i}, \hat{y_j}) z(x_i, y_j)}{\sigma_{ij}^2} \tag{6}$$

Plug equation (2) into equation (6),

$$\sum_i \sum_j \Big[\sum_k a_k w_k(\hat{x_i}, \hat{y_j}) \Big] \frac{w_l(\hat{x_i}, \hat{y_j})}{\sigma_{ij}^2} \ = \ \sum_i \sum_j \frac{w_l(\hat{x_i}, \hat{y_j}) z(x_i, y_j)}{\sigma_{ij}^2} \tag{7}$$

$$\Rightarrow \sum_k a_k \Big[\sum_i \sum_j \frac{w_l(\hat{x_i}, \hat{y_j}) w_k(\hat{x_i}, \hat{y_j})}{\sigma_{ij}^2} \Big] \ = \ \sum_i \sum_j \frac{w_l(\hat{x_i}, \hat{y_j}) z(x_i, y_j)}{\sigma_{ij}^2} \tag{8}$$

$$\Rightarrow \begin{cases} \sum_k a_k \Big[\sum_i \sum_j \frac{w_1(x_i, y_j) w_k(\hat{x_i}, \hat{y_j})}{\sigma_{ij}^2} \Big] \ = \ \sum_i \sum_j \frac{w_1(x_i, y_j) z(x_i, y_j)}{\sigma_{ij}^2} \\ \qquad \vdots \\ \sum_k a_k \Big[\sum_i \sum_j \frac{w_l(\hat{x_i}, \hat{y_j}) w_k(\hat{x_i}, \hat{y_j})}{\sigma_{ij}^2} \Big] \ = \ \sum_i \sum_j \frac{w_l(\hat{x_i}, \hat{y_j}) z(x_i, y_j)}{\sigma_{ij}^2} \\ \qquad \vdots \end{cases} \tag{9}$$

Equation system (9) can be represented in a matrix form,

$$\mathbf{WA} = \mathbf{Z} \ , \tag{10}$$

where

$$\mathbf{W} = \begin{pmatrix} W_{11} & W_{12} & \cdots \\ W_{21} & W_{22} & \cdots \\ \vdots & \vdots & \ddots \end{pmatrix} \ , \text{with} \tag{11}$$

$$W_{lk} = \sum_i \sum_j \frac{w_1(x_i, y_j) w_k(\hat{x}_i, \hat{y}_j)}{\sigma_{ij}^2} \; ; \tag{12}$$

$$\mathbf{A} = \begin{pmatrix} a_1 \\ a_2 \\ \vdots \end{pmatrix} \; ; \tag{13}$$

and

$$\mathbf{Z} = \begin{pmatrix} Z_1 \\ Z_2 \\ \vdots \end{pmatrix} \text{ , with} \tag{14}$$

$$Z_l = \sum_i \sum_j \frac{w_l(\hat{x}_i, \hat{y}_j) z(x_i, y_j)}{\sigma_{ij}^2} \; . \tag{15}$$

Solve matrix equation (10), one can obtain the fitting coefficient $\{a_k\}$.

There is one small complication for the Livingston4K beam splitter(LLO BS). Since it was tilted 45° on the yaw direction when measured, when processing this mirror, one need to rotate it back, that's to stretch the x axis $\sqrt{2}$ times. Thus for this mirror, substitute all x_i in the above formulae with $\sqrt{2}x_i$.

After obtaining the smooth structure of the phasemap, extrapolate it to the full extension of a mirror, (Fig 3). This is the base of extrapolation; the extrapolated high frequency surface aberrations will be built onto it later.

High Spatial Frequency Surface Aberration Modeling

After the separation of the low spacial frequency structure, the remaining high spacial frequency components of the measured phasemaps need to be extrapolated. There are two issues to supplement this extrapolation. One is a smoothness of the connection between the measured region and the extrapolated region. The other is the generation of the high spacial frequency component, or random noise, in the extrapolated region.

Noise Smearing

In the final phasemap with extrapolation, the measured data are retained when available. To ensure a smooth extrapolation, these measured data within $15\ (cm)$ diameter are extended to $1\ (cm)$ to outer side using the following algorithm (Fig 4):

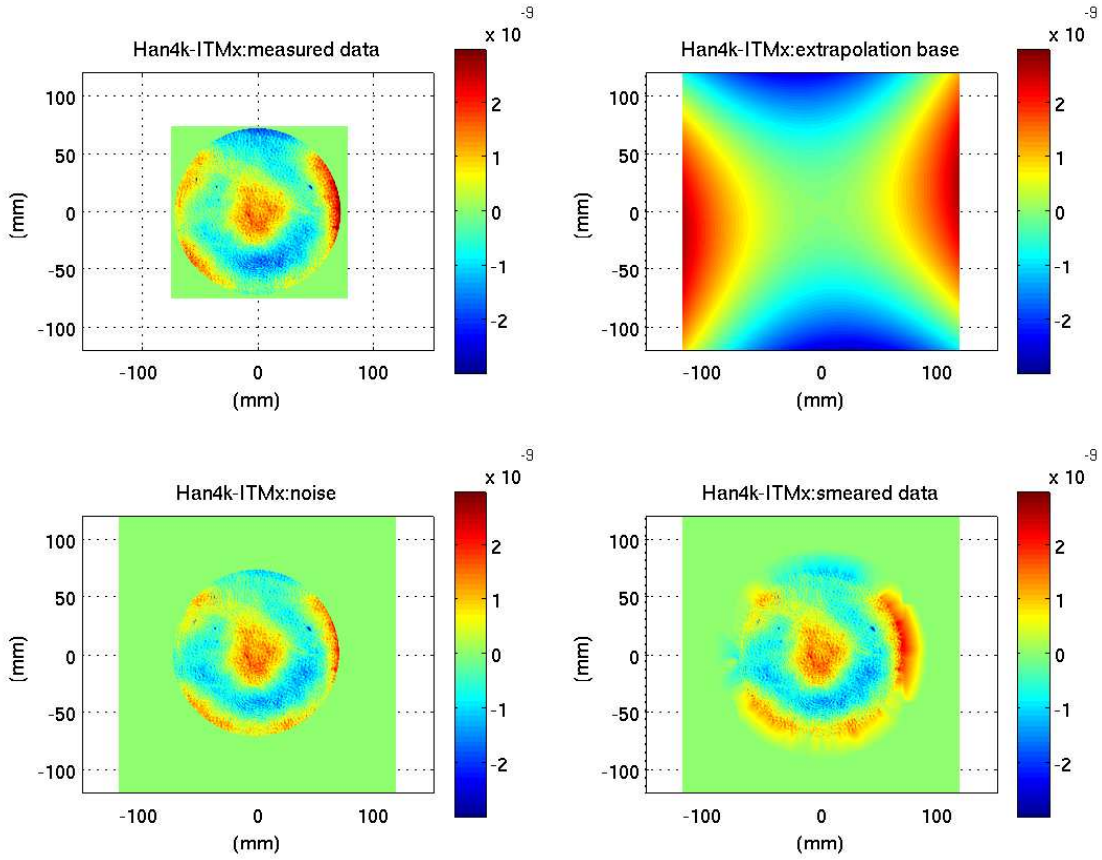

Figure 3: Example of Separation of base and noise and Smear of the noise

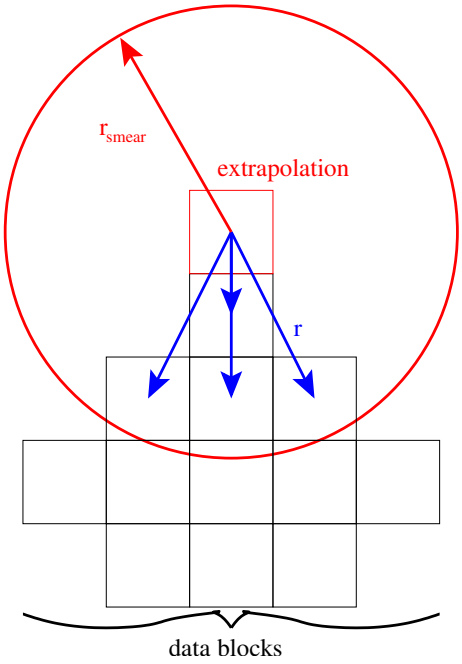

Figure 4: Scheme of smearing the noise

1. Set a radius r_{smear} so that the value of the extrapolated datum will be a weighted average of the values fall in to the circular region of r_{smear}.
2. Say the distance from the extrapolation to an existed datum block is r, then the weight assigned to the value of this datum block is $\frac{1}{(r^2+1)^2}$.
3. After adding up all the weighted values, normalize the sum, that's to divide the weighted sum by the sum of all weights, $\frac{\sum_i \frac{z(r_i)}{(r_i^2+1)^2}}{\sum_i \frac{1}{(r_i^2+1)^2}}$.
4. Apply a weight on to the smeared noise so that the noise gradually fades to zero while extending into the extrapolated region.

In that region, 1cm ring, this extraoplation based on the data averaging will have the effect that after superpose to the Zernike fit of the low frequency component, at the boundary of the measured data, the extrapolation is almost equal to the data and, at the outer boundary of the 1cm ring, it is almost equal to the Wyko polynomial based extrapolation. One resultant profile of smeared noise is shown in Fig 3.

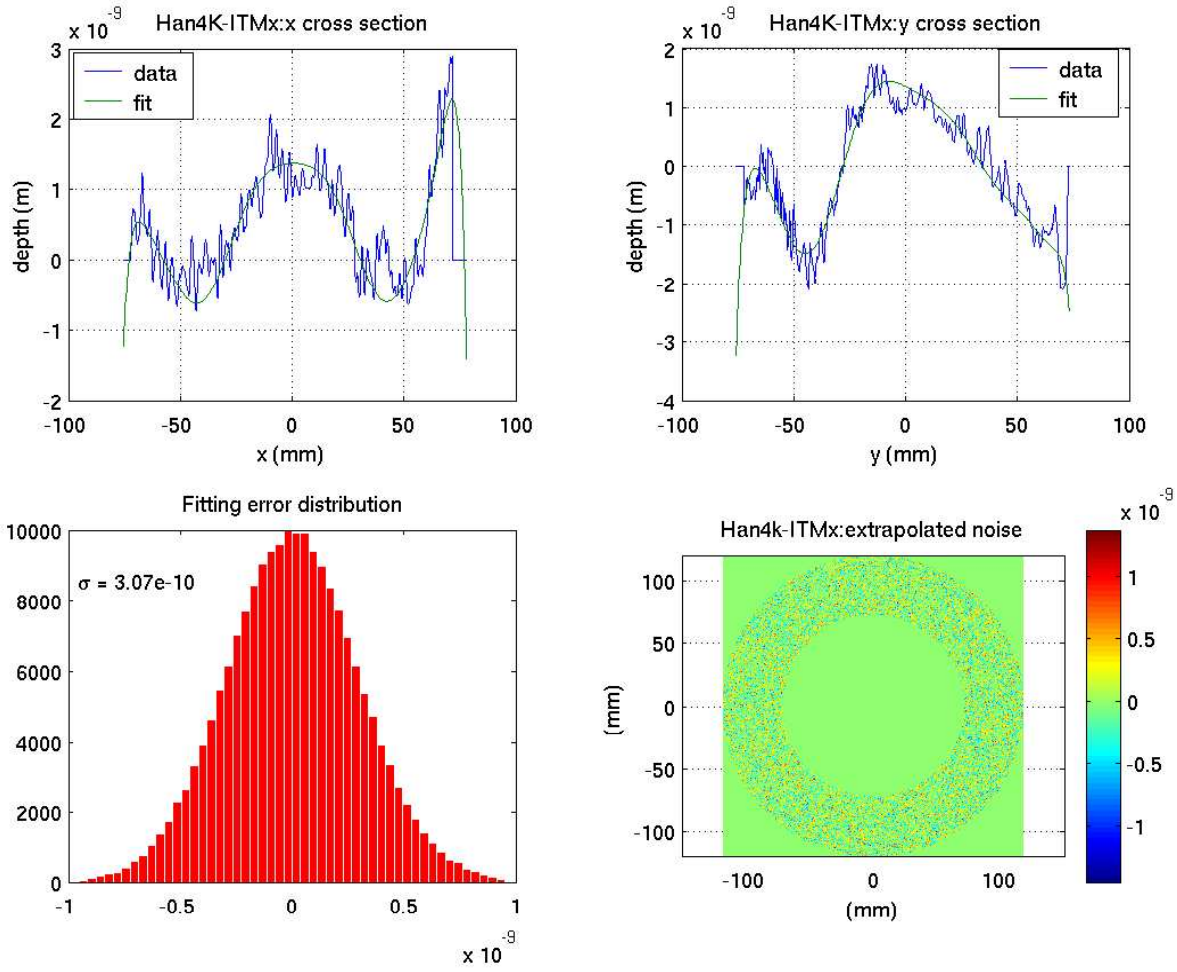

Figure 5: Example of Extrapolation of noise

Random Noise Generation

The random noise was estimated as follows. In the measured region, the residual of the data after subtracting the Wyko fit using 37 terms were fit by a gaussian form to find the width (Fig 5). The spacial frequency distribution in the frequency space is flat if random noises with this width are assigned to the data cell. By the assumption that the random noise in the extrapolated region is of the same distribution, the extrapoltated random noise is produced by a normally distributed random number generator with the mean zero and standard deviation the width obtained from above (Fig 5).

However, when comparing the extrapolated noise to the measured noise, it's apparant that the extrapolation is of much higher frequency than the measured one (Fig 6). In order to

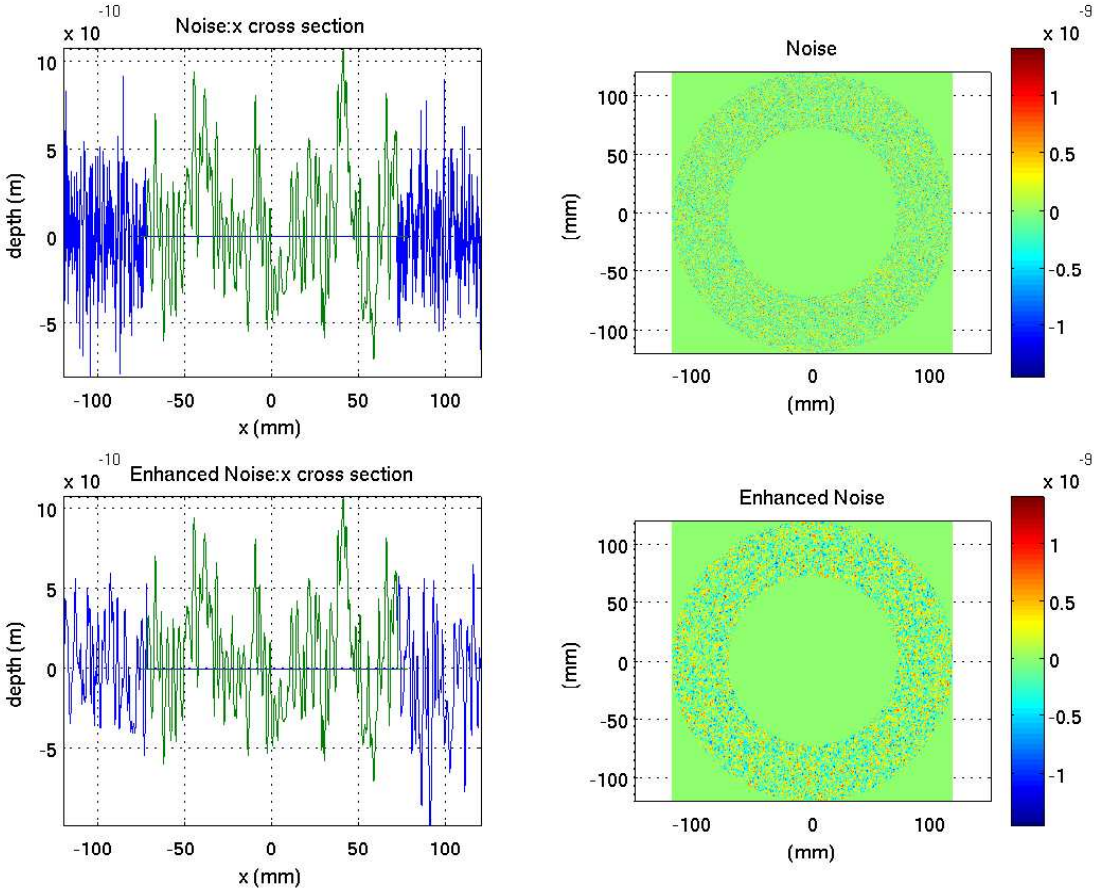

Figure 6: Example of the final noise extrapolation

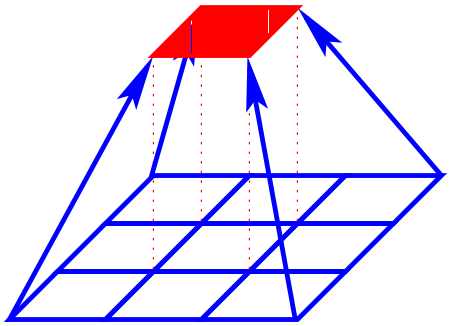

Figure 7: Scheme of integrating the noise

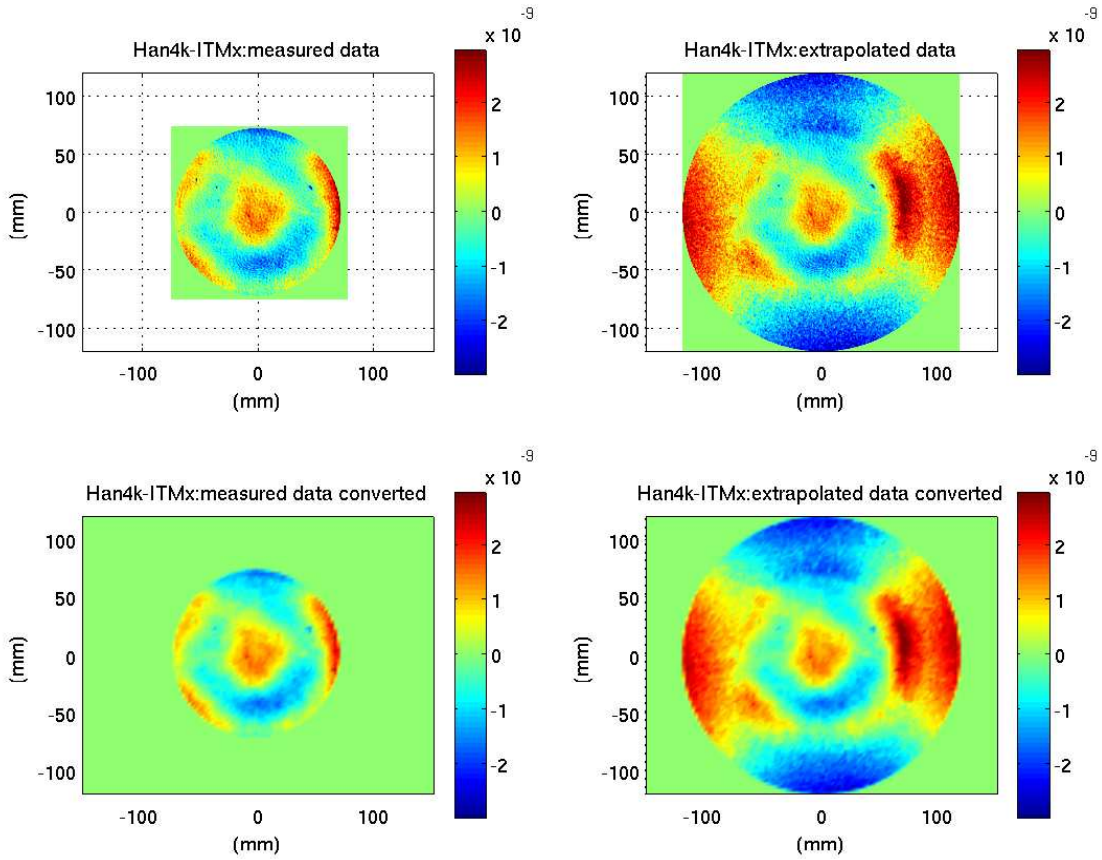

Figure 8: Example of final extrapolation and conversion

enhance the low frequency component of the extrapolation, the noise is integrated twice[4] as is described below (Fig 7):

1. For each cell in a phase-map, form a 3×3 matrix with this cell as the center and its immediate 8 neighbouring cells as the boundary.

2. Assign the mean of the values of the nine cells of the 3×3 matrix to the cell in the center.

After this process, the extrapolation becomes much closer to the measurement (Fig 6).

After superposing the extended base, the smeared measurment, and the extrapolated random noise, and setting all values outside the mirror range to be zero, the final extrapolation of the measured phase-map (Fig 8) is accomplished. After the convertion of the extrapolation by the process indicated in Fig 1, the phasemaps are but one step from being done.

Tilt Removal

The beam profile of incident laser of LIGO is Guassian, so most of the beam's power is concentrated in the central region, characterized by the diameter of this region, or Spot Size (Fig 9). Therefore, the central region, characterized by spot size, of the mirror surface is of uncomparable importance. Thus the final step of preparing a phasemap is to maximally reduce the tilts on its central region, together with piston. This task is accomplished by a Tilt Removal program, developed by B.Bochner [1].

[4]Integration has an effect to smooth function out. We can consider an simple 1-D case. For a random function $f(x)$, after Fourier decomposition, it becomes

$$f(x) = \sum_k a_k e^{ikx} \ ,$$

where k is the wave number, or spatial frequncy. After integration, it becomes

$$\int f(x)dx = \sum_k \frac{a_k}{ik} e^{ikx} \ .$$

Observe that k comes to the denominator, and therefore the smaller the frequency is, the larger the weight of this frequency becomes. Thus, the high frequency components are subdued and the low frequency components are enhanced.

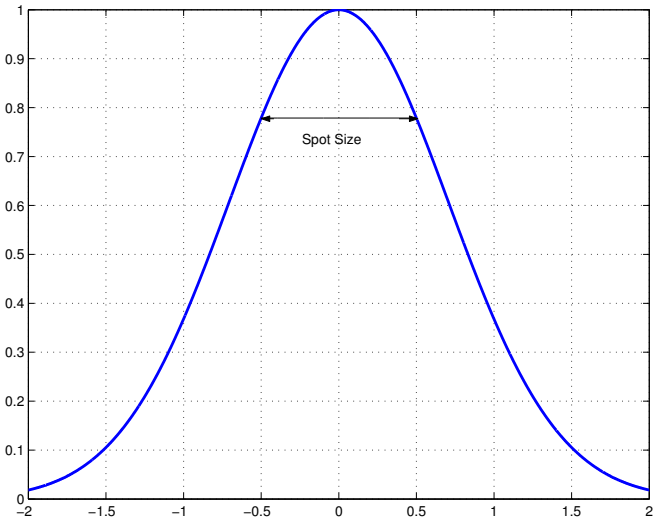

Figure 9: Profile of incident beam with its spot size

Reflection

To obtain the information of piston and tilts, first, one creates a beam of perfect TEM_{00} mode [6], characterized by the interested spot size w_0 and wavelength $\lambda = 1.064\ (\mu m)$. This beam will be impinged onto a phasemap, and the reflected beam will contain the desired information. Before that, the phasemap needs modification. Originally, the value of every cell of the phasemap is the depth, z, at this location respect to a reference plain. To accomodate the calculation of reflection, the depth z needs to be converted to phase ϕ by the following formula,

$$\phi(x, y) = e^{-i2kz(x,y)}, \text{ with} \tag{16}$$

$$k = \frac{2\pi}{\lambda}. \tag{17}$$

Multiply the modified phasemap to the incident beam, one can obtain the reflected beam profile.

Modal Decomposition

To extract the information of piston and tilts from the reflected beam profile, $Refl$, one needs to apply the technique of modal decomposition [5][6]. The basic idea is that any beam profile

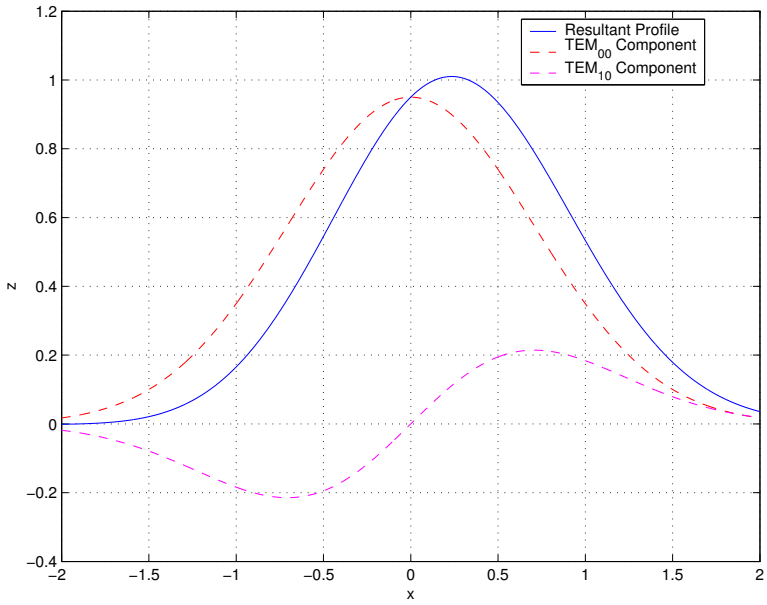

Figure 10: Example of the modal decomposition

can be described as a superposition of the Gauss-Hermite Modes, TEM$_{mn}$, as in Fig 10. Since TEM$_{mn}$ is an orthonormal base, any superposition of these modes can be decomposed by the manner similar to Fourier Decomposition.

The reflection of the incident beam can be considered as an operation on the beam. Any operation can be expressed by an operation matrix [6]:

$$\mathbf{M^{Op}} = \begin{pmatrix} M_{00,00} & M_{10,00} & M_{01,00} & \dots \\ M_{00,10} & M_{10,10} & M_{01,10} & \dots \\ M_{00,01} & M_{10,01} & M_{01,01} & \dots \\ \vdots & \vdots & \vdots & \ddots \end{pmatrix}, \text{with} \tag{18}$$

$$M_{nm,kl} = \int_{-\infty}^{\infty} TEM_{nm}(x,y,z)^* \mathbf{Op}[TEM_{kl}(x,y,z)]dxdy, \tag{19}$$

where A^* is the complex conjugate of A. Since the misalignments are very slight, the greatest effect are in the modes of the lowest order. Thus, all one needs to do is to check the first 3 modes, TEM$_{00}$, TEM$_{01}$, and TEM$_{10}$. And therefore, the operation matrix will be simplified to,

$$\mathbf{M^{Op}} = \begin{pmatrix} M_{00,00} & M_{10,00} & M_{01,00} \\ M_{00,10} & M_{10,10} & M_{01,10} \\ M_{00,01} & M_{10,01} & M_{01,01} \end{pmatrix}. \tag{20}$$

When one apply the matrix in (20) to an incident beam of TEM_{00} mode, the following will be obtained,

$$\begin{aligned}
\mathbf{Op}[TEM_{00}] &= \begin{pmatrix} M_{00,00} & M_{10,00} & M_{01,00} \\ M_{00,10} & M_{10,10} & M_{01,10} \\ M_{00,01} & M_{10,01} & M_{01,01} \end{pmatrix} \begin{pmatrix} a_{00} \\ a_{10} \\ a_{01} \end{pmatrix} \\
&= \begin{pmatrix} M_{00,00} & M_{10,00} & M_{01,00} \\ M_{00,10} & M_{10,10} & M_{01,10} \\ M_{00,01} & M_{10,01} & M_{01,01} \end{pmatrix} \begin{pmatrix} 1 \\ 0 \\ 0 \end{pmatrix} \\
&= \begin{pmatrix} c_{00} \\ c_{10} \\ c_{01} \end{pmatrix} , \qquad (21)
\end{aligned}$$

where a_{nm} is the coefficient of TEM_{nm} component in the incident beam; c_{nm} is the coefficient of TEM_{nm} component in the reflected beam.

Piston

The information of piston, d, can be extracted from the coefficient of TEM_{00} mode. Suppose one can write the phasemap $z(x, y)$ as the superposition of a series *Zernike Polynomials*, $\{Z_{nm}(x, y)\}$[4] as

$$z(x, y) = \sum_{n,m} a_{nm} Z_{nm}(x, y) \, , \qquad (22)$$

where $a_{00}Z_{00} = a_{00} \times 1 = a_{00} = d$. Then by equation (16), the reflection beam is

$$Refl = TEM_{00} e^{-i2kz(x,y)} = TEM_{00} e^{-i2k \sum_{n,m} a_{nm} Z_{nm}(x,y)}. \qquad (23)$$

Assume that the dominant effect comes from the lowest order of Zernike polynomials, then equaiton (23) can be simplified as

$$Refl \approx TEM_{00} e^{-i2ka_{00}Z_{00}(x,y)} = TEM_{00} e^{-i2kd}. \qquad (24)$$

Thus, in order to extract information of piston, we need to do the following,

$$\begin{aligned}
c_{00} &= \int Refl \cdot TEM_{00}^{*} dxdy \\
&= \int TEM_{00} e^{-i2kd} \cdot TEM_{00}^{*} dxdy \\
&= e^{-i2kd} \int TEM_{00} \cdot TEM_{00}^{*} dxdy \\
&= Ae^{i\alpha} \qquad (25) \\
\Rightarrow d &= \frac{\alpha}{-2k} \qquad (26)
\end{aligned}$$

where k is the wave number which defined in equation (17).

Tilts

The information of tilts, tilt on the pitch direction θ_X and tilt on the yaw direction θ_Y, can be extracted from the TEM_{01} and TEM_{10} respectively. Say if the mirror tilts θ_X on the pitch direction and θ_Y on the yaw direction, when the incident beam impinges from the front surface of the mirror, the operational matrix for the reflected beam is [5]:

$$\mathbf{M^{Op}} = \begin{pmatrix} 1 & -2i\hat{\Theta}_Y & 2i\hat{\Theta}_X \\ -2i\hat{\Theta}_Y & 1 & 0 \\ 2i\hat{\Theta}_X & 0 & 1 \end{pmatrix} \ ^{5}, \tag{27}$$

with

$$2\hat{\Theta}_{X(Y)} = 2\pi w \sin\theta_{X(Y)}/\lambda = wk \sin\theta_{X(Y)} \ , \tag{28}$$

where w is the spot size and k is the wave number. Apply matrix (27) to the incident TEM_{00} beam, one will obtain

$$\begin{pmatrix} 1 & -2i\hat{\Theta}_Y & 2i\hat{\Theta}_X \\ -2i\hat{\Theta}_Y & 1 & 0 \\ 2i\hat{\Theta}_X & 0 & 1 \end{pmatrix} \begin{pmatrix} 1 \\ 0 \\ 0 \end{pmatrix} = \begin{pmatrix} 1 \\ -2i\hat{\Theta}_Y \\ 2i\hat{\Theta}_X \end{pmatrix} \tag{29}$$

Clearly, the information of the tilts will be contained in the imaginary part of the coefficients of the reflected beam's TEM_{nm} components.

Thus, θ_X andθ_Y, can be extracte by the following fomulae:

$$c_{01} = \int Refl \cdot TEM_{01}^{*} dxdy = Re_{01} + iIm_{01} \tag{30}$$

$$\Rightarrow \theta_X = \frac{\sin^{-1} Im_{01}}{wk} \tag{31}$$

$$c_{10} = \int Refl \cdot TEM_{10}^{*} dxdy = Re_{10} + iIm_{10} \tag{32}$$

$$\Rightarrow \theta_Y = \frac{\sin^{-1} Im_{10}}{-wk} \ ^{6} \tag{33}$$

where w is the spot size.

---

[5] In expression (27), all higher order terms of $\hat{\Theta}_{X(Y)}$ are neglected.

[6] In the Tilt Removal program,the calculation of θ_Y uses a slightly different formula, $\theta_Y = \frac{\sin^{-1} b_{10}}{-wk\cos\theta_X}$. That's because while untilting the mirror on the pitch direction, the amount of tilt on the yaw direction is changed, since the hight function z at (x, y) due to the tilt is $z(x, y) = x\sin\theta_X + (y\cos\theta_X)\sin\theta_Y$[1].

However, with θ_X being so small, the extra $\cos\theta_X$ hardly contribute any substantial difference from the results calculated by equation (33).

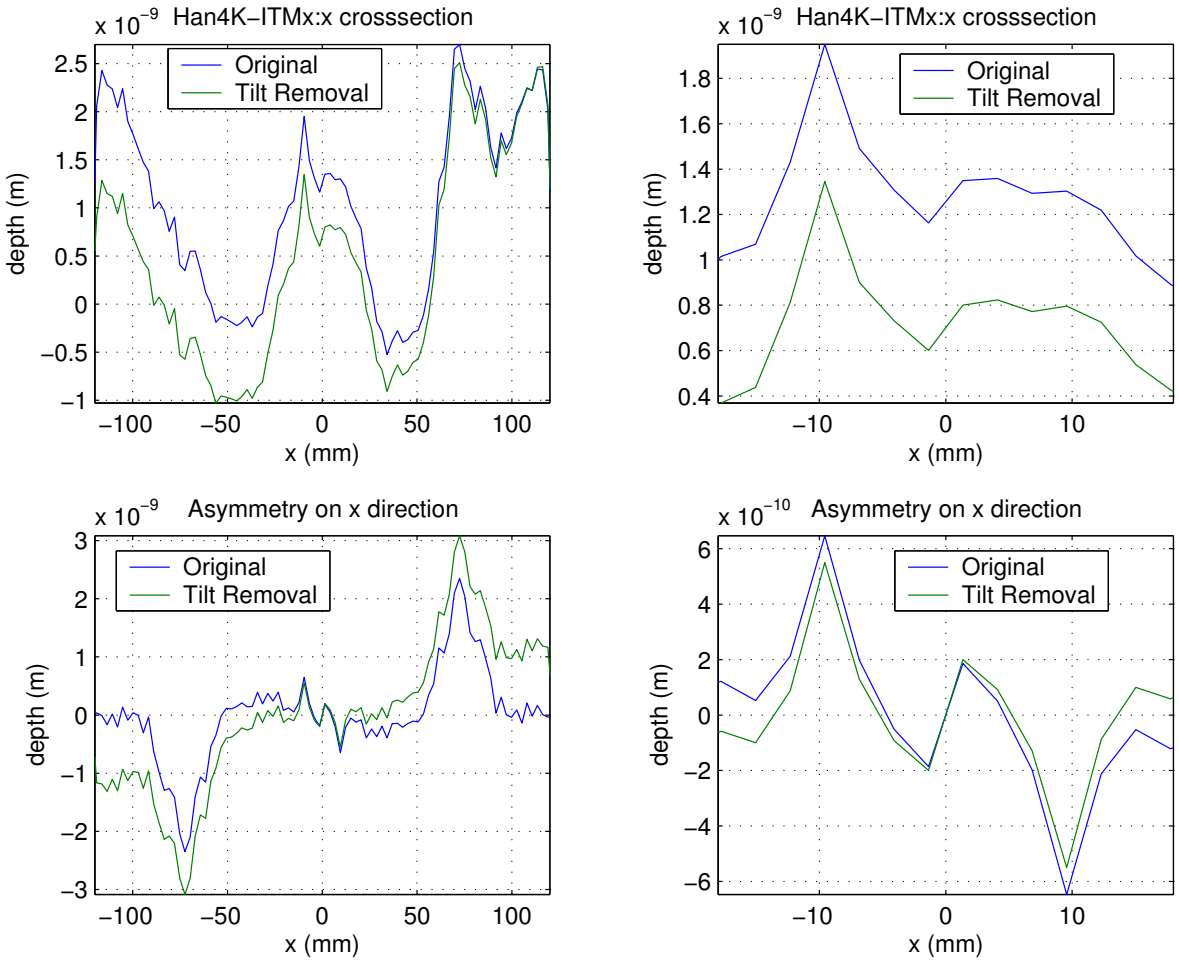

Figure 11: Example of the effect of tilt removal

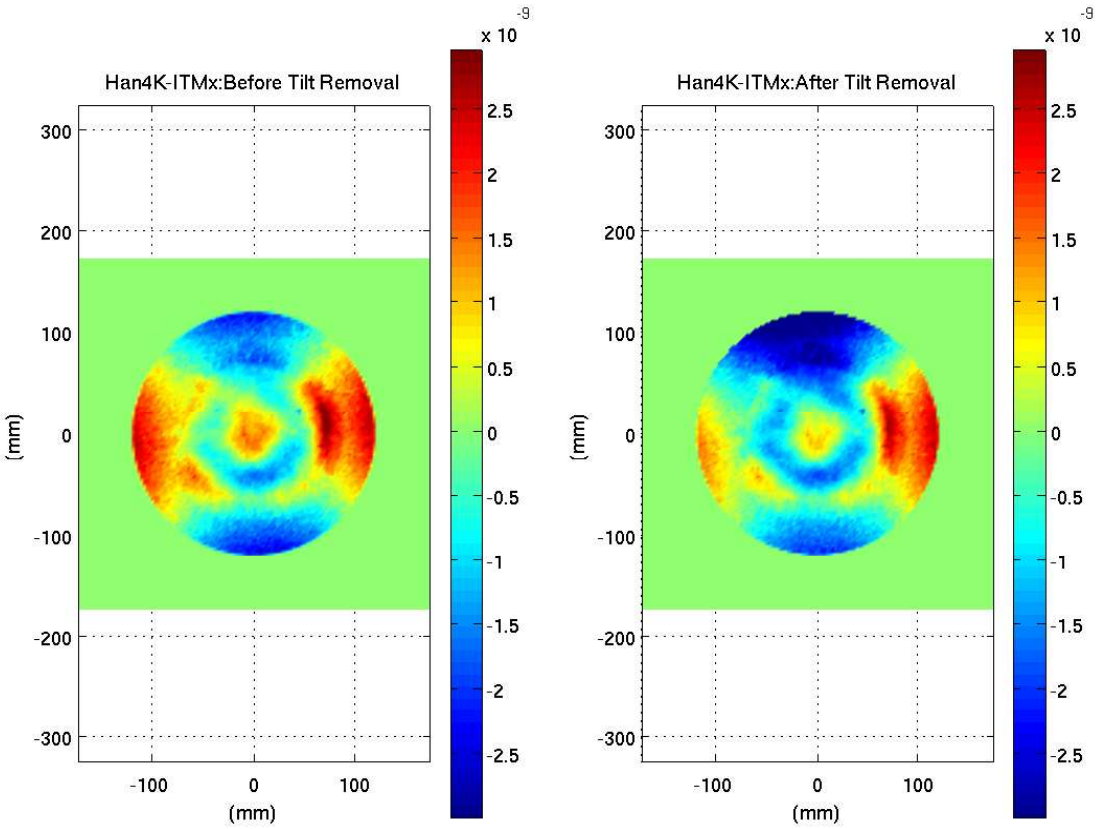

Figure 12: Example of final input phasemap to FFT program

After obtaining the piston and tilts, one can adjust the phasemap accordingly. The effect of the Tilt Removal process is indicated in Fig 11. The plots in the first row are the comparison of the phasemaps' x crosssection, which indicate that the piston is indeed somewhat removed. The plots in the second row are the comparison of the x crosssection of the odd components of the phasemaps. The plot in the first column seems to indicated that after tilt removal, the entire phasemap seems to tilt even more than the original; however, as the plot in the second column indicated, the surface within the range characterized by spot size has less tilt, or its odd components are minimized.

After this last step (Fig 12), the phasemaps are finally ready to be input to the FFT Program.

Reference

1. B. Bochner, *Modelling the Performance of Interferometric Gravitational-Wave Detectors with Realistically Imperfect Optics*, LIGO-P980004-00-R

2. G. Billingsley,

   `www.ligo.caltech.edu/~gari/COCAsBuilt.htm`

3. R. Dodda, *Impact of Imperfect Optics on the Performance of Laser Interferometer Gravitational Wave Observatory (LIGO)*, 2003

4. M. Born and E. Wolf, *Principles of Optics*, 1959

5. B. Bhawal, M. Evans, M. Rakhmanov and H. Yamamoto, *Time Domain Modal Model in End-to-End simulation package*, LIGO-T009981-03-E, 2004

6. M. Eichenfield, *Modelling and Commissioning the Wavefront Sensing Auto-Alignment System of a Triangular Mode Cleaner Cavity*, LIGO-T030234-00-D

7. B. Bhawal, X. Xu,and H. Yamamoto, *Effects of As-Built Mirror Aberrations (I)*, LIGO-T040173-04-E, 2004